Engineering Science and Technology, an International Journal xxx (2017) xxx–xxx

HOSTED BY

ELSEVIER

Contents lists available at ScienceDirect

Engineering Science and Technology, an International Journal

journal homepage: www.elsevier.com/locate/jestch

Full Length Article

A simple overlap angle control strategy for reducing commutation torque ripple in a brushless DC motor drive

Chetan K. Lad *, R Chudamani

Department of Electrical Engineering, Sardar Vallabhbhai National Institute of Technology, Surat 395007, India

ARTICLE INFO

Article history:
Received 25 February 2017
Revised 19 September 2017
Accepted 22 September 2017
Available online xxxx

Keywords:
Commutation torque ripple
brushless DC motor
Direct torque control
Twelve voltage space vector
Overlap angle control, inverter losses

ABSTRACT

A commutation torque ripple is generated in a brushless DC motor due to a finite time taken for current transfer between outgoing phase and incoming phase due to the phase inductance. The effect of commutation ripple will be more severe for low voltage high current BLDC drives used for automotive applications. Direct Torque Control (DTC) techniques are used to reduce the torque ripple. Two phase conduction with six voltage space vectors and three phase conduction with twelve voltage space vectors with DTC are used to reduce the torque ripple. Twelve Step DTC (TSDTC) is capable of reducing torque ripple considerably but at the cost of increased inverter and winding losses. In Six Step DTC (SSDTC) the torque ripple is higher than that of TSDTC but with reduced winding and inverter losses. In this paper an attempt has been made to strike a balance between torque ripple and losses. A novel Direct Torque Control with twelve voltage space vector with overlap angle control has been proposed. The proposed method is validated through simulation and experimental results.

1. Introduction

Brushless DC (BLDC) motors are widely used due to their advantages such as better power/weight and torque/current ratio compared to Permanent Magnet Synchronous Motor (PMSM) [1]. The torque ripple is mainly due to Pulse Width Modulation (PWM), non-ideal trapezoidal back-EMF and commutation between outgoing and incoming phases [2]. Torque ripple due to PWM can be taken care of by the rotor inertia but the commutation torque ripple is greater in magnitude and severely affects the motor performance. Commutation torque ripple is due to finite transition time between outgoing phase current to incoming phase current due to winding inductance [3,4]. The commutation torque ripple produces adverse effect, reduces reliability of the BLDC drive and the relevant studies are reported in [3–5]. Various current control techniques are used to minimize torque ripple, by deriving shape function [2], controlling DC link current [2] and controlling common DC signal current [6]. An attempt has been made by Song and Choy to control commutation torque ripple by using DC link current as discussed [7]. In the above work the time-derivative of outgoing and incoming phase current is utilized to calculate duty ratio to control commutation interval. The effect of DC link voltage, back-EMF and phase current on commutation is analysed in [8]. It has been stated that when phase back-EMF is higher than one fourth of the DC link voltage the control in phase current cannot compensate effect on torque pulsation during commutation. The generation of torque ripple during phase commutation is mathematically analysed in [9,10]. The influence of commutation time on torque ripple and the relation between commutation time and speed have been analysed. The commutation time is determined using detection and comparator circuits. The commutation torque ripple reduction using PWM techniques and without using commutation time calculation is discussed in [11]. A control strategy for speed control of SRM drive along with torque ripple reduction has been proposed in [12]. Minimization in torque ripple is attempted by controlling current profile and by selecting suitable turn on and turn off angles. The effect of hybrid switching conduction on commutation torque ripple for 120° and 180° conduction mode has been analysed in [13] for various operating speeds. The idea to equalize the mismatched time of two commutating phase currents during commutation interval is discussed and analysed in [14] for low and high speed motor operation. The detailed analysis of commutation torque ripple due to phase current is presented in [15]. It has been concluded that the commutation torque ripple is not only dependent on variation in current but also on increase in speed. In [16], the detailed expressions of variation in torque under non-commutation and commutation period have been deduced. The torque variation rate is analysed and the opti-

* Corresponding author.
E-mail address: chetan.lad@ckpcet.ac.in (C.K. Lad).
Peer review under responsibility of Karabuk University.

https://doi.org/10.1016/j.jestch.2017.09.005
2215-0986/

mization in switching vector selection is discussed based on sign of variation in torque ripple to reduce commutation torque ripple and torque ripple due to non-ideal back-EMF. The method has been proposed in [17] to measure commutation interval from terminal voltage and to calculate pwm duty ratio to suppress commutation torque ripple. Lu et al. proposed a method to reduce torque ripple of BLDC motor with nonideal back EMF [18] based on duty ratio calculation by ignoring diode freewheeling of the inactive phase. Several works have been reported regarding commutation torque ripple.

The direct torque control (DTC) emerged as a solution for these problems and it was originally developed for the control of induction motor drives in which direct control of flux and electromagnetic torque was attempted. It utilized the estimated flux and electromagnetic torque to derive optimal inverter switching to obtain fast response. The DTC for PMSM has been introduced in [19]. The DTC of BLDC motor differs from that of the induction motor and PMSM due to non-sinusoidal back-EMF. Based on the characteristics of BLDC, the hybrid conduction mode is introduced to reduce torque ripple in [20,21]. For direct torque control it is important that the estimated torque is accurate. The direct self controlled method for BLDC by utilizing stator flux linkage reference with three phase conduction is discussed in [22]. The rounding effect in phase back-EMF is one of the cause for torque ripple production, the back-EMF is derived by using shape function in [23] for torque estimation.

The DTC scheme for BLDC motor drives to reduce low-frequency torque ripple and obtain fast torque response is discussed in [21]. It has been observed that there are dips in flux amplitude at every 60 electrical degrees due to commutation. The effect of applying zero voltage space vector in DTC of permanent magnet machine is not same as that in induction motor. It is due to the effect of permanent magnet and is discussed by Zhong and Rahman in [19]. Since magnets are rotating, the vector of stator flux linkage will change even when the zero voltage vectors are selected. Thus the stator flux linkage vector in a permanent magnet motor cannot be controlled by the zero voltage vector. It is discussed in [24] that the use of zero voltage vector decreases the torque slowly in permanent magnet motor compared to induction motor. The DTC of BLDC motor by using accelerating-decelerating vectors is suggested by Ozturk and Toliyat in [25]. The DTC using 12 voltage space vector for alternate two and three phase conduction is discussed in [26]. Though torque ripple is controlled in this method, switching losses in the inverter and winding losses are increased. Torque ripple reduction by using three level hysteresis torque controller is discussed in [27]. The use of three level hysteresis controller results into a complex algorithm for selecting the vectors that are to be switched.

The torque ripple is appreciably high with six voltage space vector and two phase conduction and it is reduced by using twelve voltage space vectors but at the cost of increased inverter and winding losses. In three phase conduction control method the duration for which three switches conduct simultaneously is 30 electrical degrees. This duration of three phase conduction is called overlap region and it is given by $2\theta_{ov}$ where θ_{ov} is the overlap angle. Keeping the overlap angle ' θ_{ov} ' equal for all load currents in TSDTC, results in increased inverter and winding losses. An attempt has been made to reduce torque ripple as well as inverter and winding losses by choosing ' θ_{ov} ' as a function of load and speed.

In this paper a Direct Torque Control technique to reduce the commutation torque ripple has been proposed. This method is essentially the twelve voltage space vector technique with overlap angle control. Conduction of three devices simultaneously for fixed duration of 30° in-between two consecutive sectors of 60° is discussed in [26] to reduce commutation torque ripple. An attempt has been made in this work for reducing the commutation torque ripple but at the same time trying to reduce the conduction period of three devices to limit the inverter and winding losses. In the proposed method the duration for which three devices conduct simultaneously is not fixed but varies with speed and load. The overlap angle is determined using lookup table based on speed and load. In this paper for the convenience of explanation, two phase conduction DTC using six switching space vector has been abbreviated as SSDTC (Six Step DTC) and combined two phase - three phase conduction DTC using twelve switching space vector as TSDTC (Twelve Step DTC). The performance of the drive for the proposed method is analysed with various load conditions and the results are presented.

2. Proposed DTC with overlap angle control

BLDC motor is basically operated in two phase conduction mode, but with two phase conduction commutation torque ripple is produced during transition between incoming phase and outgoing phase. During commutation, transient torque is developed because the sum of the two commutating current is rarely constant. If back-EMFs are assumed constant and equal in magnitude, as well as speed of the motor is assumed to be constant then the pulsating torque will be zero if,

$$|i_b + i_c| = i_a = I_{av} \tag{1}$$

Unfortunately due to winding inductance, the sum of commutating current is never constant and hence commutation ripple is produced. The commutation torque ripple can be reduced by maintaining the sum of the current from outgoing phase to incoming phase constant and equal to I_{av}. This can be achieved by three phase conduction of BLDC motor during commutation. The adverse effect of commutation is observed on motor performance when the motor is fully loaded and run at high speed. The TSDTC method discussed in [26] to reduce commutation torque ripple uses alternately two and three phase conduction. The switching losses in the inverter are more as three phases are switched on simultaneously for 30° irrespective of load. Also the copper losses in the winding are higher due to increase in phase conduction to 150° compared to 120° in SSDTC. In the proposed method the drive is operated in the three phase conduction only for duration of $2\theta_{ov}$ where θ_{ov} is the overlap angle and it varies with speed and load. It is low for lightly loaded and low/medium speed condition; the operation is more close to SSDTC with reduced torque ripple.

The schematic diagram of the proposed method of DTC of BLDC is shown in Fig. 1. The proposed method is implemented in the following sequence: (i) flux linkage estimation (ii) torque estimation (iii) determination of overlap angle 'θ_{ov}' (iv) identification of overlap and non-overlap region using θ_{ov} (v) selection of switching space vector. These are explained in subsequent sub-sections.

2.1. Flux linkage estimation for BLDC drive

The phase back-EMF cannot be easily obtained in a BLDC motor due to non availability of neutral terminal. Thus line-to-line terminal voltages are utilized to determine $v_{s\alpha}$ and $v_{s\beta}$ using Clarke transformation. The line-to-line Clarke transformation to obtain $v_{s\alpha\beta}$ from $v_{ab-bc-ca}$ is derived from Fig. 2 using Eqs. (2)–(6).

$$v_{s\alpha} = \frac{2}{3\sqrt{3}}[v_{ab}\cos 30^\circ - v_{ca}\cos 30^\circ] \tag{2}$$

$$v_{s\alpha} = \frac{1}{3\sqrt{3}}[\sqrt{3}v_{ab} - \sqrt{3}v_{ca}] \tag{3}$$

Please cite this article in press as: C.K. Lad, R. Chudamani, A simple overlap angle control strategy for reducing commutation torque ripple in a brushless DC motor drive, Eng. Sci. Tech., Int. J. (2017), https://doi.org/10.1016/j.jestch.2017.09.005

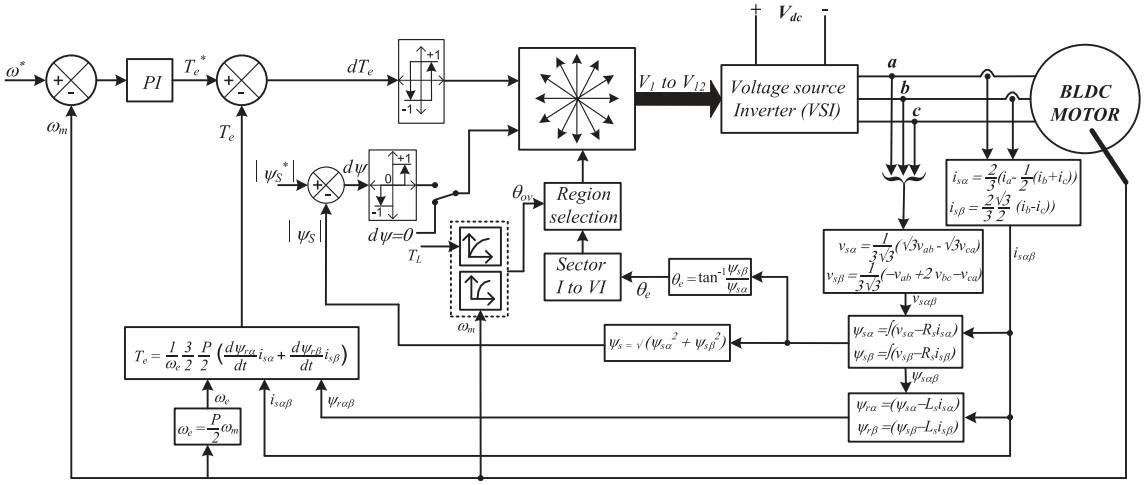

Fig. 1. Schematic diagram of proposed overlap angle controlled DTC of BLDC motor.

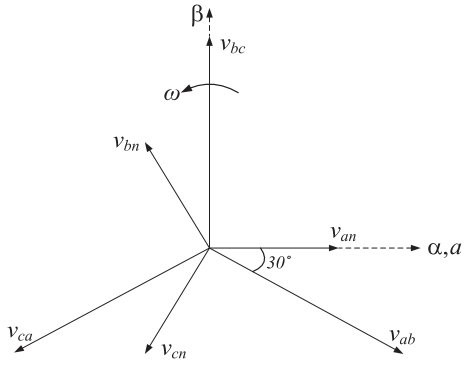

Fig. 2. Phasor diagram for line to line Clarke transformation.

$$v_{s\beta} = \frac{2}{3\sqrt{3}}[-v_{ab}\sin 30^\circ + v_{bc} - v_{ca}\sin 30^\circ] \tag{4}$$

$$v_{s\beta} = \frac{1}{3\sqrt{3}}[-v_{ab} + 2v_{bc} - v_{ca}] \tag{5}$$

Putting (3) and (5) in the matrix form we get,

$$\begin{bmatrix} v_{s\alpha} \\ v_{s\beta} \end{bmatrix} = \frac{1}{3\sqrt{3}} \begin{bmatrix} \sqrt{3} & 0 & -\sqrt{3} \\ -1 & 2 & -1 \end{bmatrix} \begin{bmatrix} v_{ab} \\ v_{bc} \\ v_{ca} \end{bmatrix} \tag{6}$$

In relation with DTC of PMSM drives [24] the electromagnetic torque and flux linkages for DTC of nonsinusoidal back-EMF machine is discussed and derived in [20]. The stator flux linkage vector can be obtained from the transformed stator voltages $v_{s\alpha\beta}$ and transformed stator currents $i_{s\alpha\beta}$ as,

$$v_{s\alpha} = R_s i_{s\alpha} + L_s \frac{di_{s\alpha}}{dt} + \frac{d\psi_{r\alpha}}{dt} \tag{7}$$

$$v_{s\beta} = R_s i_{s\beta} + L_s \frac{di_{s\beta}}{dt} + \frac{d\psi_{r\beta}}{dt} \tag{8}$$

Integrating (7) and (8) we get,

$$\int (v_{s\alpha} - R_s i_{s\alpha})dt = \int \left(L_s \frac{di_{s\alpha}}{dt} + \frac{d\psi_{r\alpha}}{dt}\right)dt = L_s i_{s\alpha} + \psi_{r\alpha} \tag{9}$$

$$\int (v_{s\beta} - R_s i_{s\beta})dt = \int \left(L_s \frac{di_{s\beta}}{dt} + \frac{d\psi_{r\beta}}{dt}\right)dt = L_s i_{s\beta} + \psi_{r\beta} \tag{10}$$

Further relation between stator flux linkages and rotor flux linkages are given by,

$$\psi_{r\alpha} = (\psi_{s\alpha} - L_s i_{s\alpha}) \tag{11}$$

$$\psi_{r\beta} = (\psi_{s\beta} - L_s i_{s\beta}) \tag{12}$$

By substituting (11) and (12) into (9) and (10) respectively we obtain,

$$\psi_{s\alpha}(t) = \int (v_{s\alpha} - R_s i_{s\alpha})dt \tag{13}$$

$$\psi_{s\beta}(t) = \int (v_{s\beta} - R_s i_{s\beta})dt \tag{14}$$

The stator flux linkages can be estimated using (13) and (14). The command vector of stator flux linkage is given by,

$$\psi_s^* = \psi_{s\alpha} + j\psi_{s\beta} \tag{15}$$

The magnitude of stator flux linkage can be calculated by,

$$|\psi_s^*| = \sqrt{\psi_{s\alpha}^2 + \psi_{s\beta}^2} \tag{16}$$

The electrical rotor angle θ_e can be calculated from (15) and (16) as,

$$\theta_e = tan^{-1}\left(\frac{\psi_{s\beta}}{\psi_{s\alpha}}\right) \tag{17}$$

Here stator flux linkage $|\psi_s^*|$ varies with electrical rotor position, unlike the flux vector in PMSM machines with sinusoidal back-EMF as discussed in [21]. Thus during commutation in two phase conduction of BLDC motor, the locus of the tip of the flux vector is not smooth.

2.2. Torque estimation

The torque expression for PMSM with sinusoidal/nonsinusoidal back-EMF in synchronously rotating *d-q* reference frame by neglecting the effect of mutual inductance is expressed as,

$$T_e = \frac{3p}{4}\left[\left(\frac{dL_{ds}}{d\theta_e}i_{sd} + \frac{d\psi_{rd}}{d\theta_e} - \psi_{sq}\right)i_{sd} + \left(\frac{dL_{qs}}{d\theta_e}i_{sq} + \frac{d\psi_{rq}}{d\theta_e} + \psi_{sd}\right)i_{sq}\right] \tag{18}$$

where,

$$\psi_{sd} = L_{ds}i_{sd} + \psi_{rd} \tag{19}$$

$$\psi_{sq} = L_{qs}i_{sq} + \psi_{rq} \tag{20}$$

Please cite this article in press as: C.K. Lad, R. Chudamani, A simple overlap angle control strategy for reducing commutation torque ripple in a brushless DC motor drive, Eng. Sci. Tech., Int. J. (2017), https://doi.org/10.1016/j.jestch.2017.09.005

For non-sinusoidal flux distribution in BLDC motor $\frac{d\psi_{rd}}{d\theta_e} \neq 0$ and $\frac{d\psi_{rq}}{d\theta_e} \neq 0$. Since L_{ds}, L_{qs} are considered constant for nonsalient pole machines, the electromagnetic torque equation (18) can be simplified for BLDC motor as,

$$T_e = \frac{3p}{4}\left[\left(\frac{d\psi_{rd}}{d\theta_e} - \psi_{sq}\right)i_{sd} + \left(\frac{d\psi_{rq}}{d\theta_e} + \psi_{sd}\right)i_{sq}\right] \tag{21}$$

Synchronous reference frame stator flux linkages ψ_{rd} and ψ_{rq} in (21) are related to stationary reference frame rotor flux linkages $\psi_{r\alpha}$ and $\psi_{r\beta}$ as,

$$\psi_{r\alpha} = \psi_{rd}cos\theta_e - \psi_{rq}sin\theta_e \tag{22}$$

$$\psi_{r\beta} = \psi_{rd}sin\theta_e + \psi_{rq}cos\theta_e \tag{23}$$

Rotor flux linkages $\psi_{r\alpha}$ and $\psi_{r\beta}$ are estimated from stator flux linkages $\psi_{s\alpha}$ and $\psi_{s\beta}$ as given in (11) and (12). Differentiating (22) and (23) with respect to θ_e and substituting in (21) give a simplified torque equation in α-β reference frame for BLDC motor as,

$$T_e = \frac{3p}{4}\left(\frac{d\psi_{r\alpha}}{d\theta_e}i_{s\alpha} + \frac{d\psi_{r\beta}}{d\theta_e}i_{s\beta}\right) \tag{24}$$

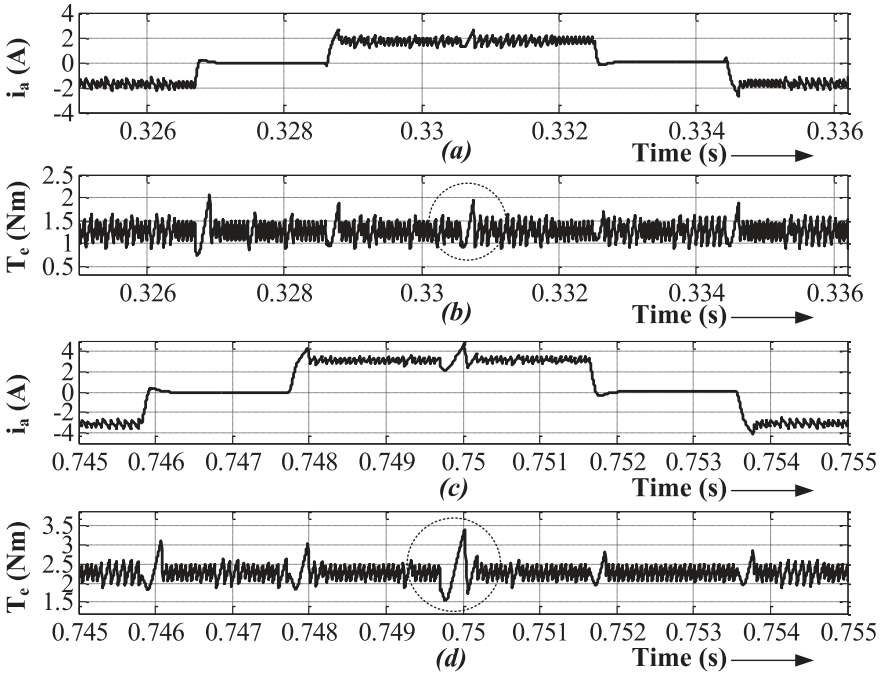

Fig. 3. Study of effect of commutation on phase current and electromagnetic torque for different load at 270 r/s for SSDTC (a) and (b) at 1 Nm load, (c) and (d) at 2 Nm load.

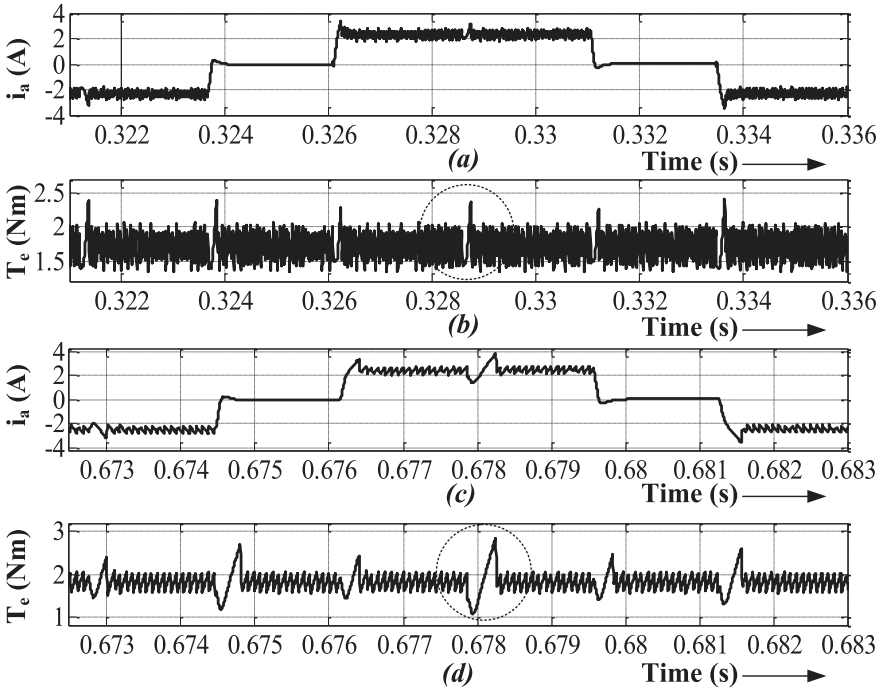

Fig. 4. Study of effect of commutation on phase current and electromagnetic torque for different speed at 1.5 Nm load for SSDTC (a) and (b) at 213 r/s, (c) and (d) at 308 r/s.

Please cite this article in press as: C.K. Lad, R. Chudamani, A simple overlap angle control strategy for reducing commutation torque ripple in a brushless DC motor drive, Eng. Sci. Tech., Int. J. (2017), https://doi.org/10.1016/j.jestch.2017.09.005

As the electrical speed ω_e of the rotor is given by $\frac{d\theta_e}{dt}$, (24) can be deduced to (25),

$$T_e = \frac{3p}{4}\frac{1}{\omega_e}\left(\frac{d\psi_{r\alpha}}{dt}i_s + \frac{d\psi_{r\beta}}{dt}i_{s\beta}\right) \tag{25}$$

2.3. Determination of overlap angle θ_{ov}

The commutation torque ripple is analysed for wide range of load for different speed operation and vice versa for SSDTC. Then optimum overlap angle is determined by trial and error to suppress the commutation torque ripple to PWM ripple or that produced in TSDTC. Finally lookup tables are prepared based on speed and load to determine optimum overlap angle. The details of the analysis are produced in further explanation.

The armature current and electromagnetic torque of the motor during the commutation interval is observed at same speed for the different loads using SSDTC. Fig. 3(a) and (c) show phase 'a' current at the same speed of 270 r/s at 1 Nm and 2 Nm load respectively. The effect of commutation on armature current with 2 Nm load operation is worse compared to 1 Nm load operation. The effect of this commutating current is clearly observed on electromagnetic torque encircled in Fig. 3(b) and (d). The commutation torque ripple ΔT_e increases from 1.03 Nm to 1.9 Nm as shown in Fig. 3 (b) and (d) respectively.

Similar study has been carried out for a given load and different speed operation using SSDTC. The effect of commutation in armature current with high speed operation is worse compared to low

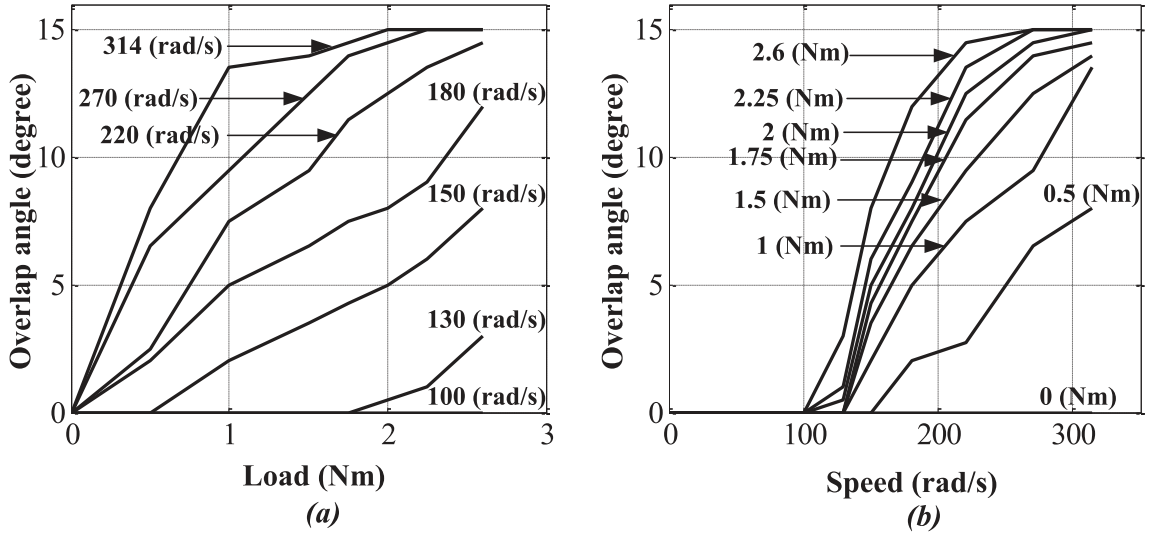

Fig. 5. Optimum overlap angle to suppress commutation torque ripple within the PWM torque ripple (a) for different load operation (b) for different speed operation.

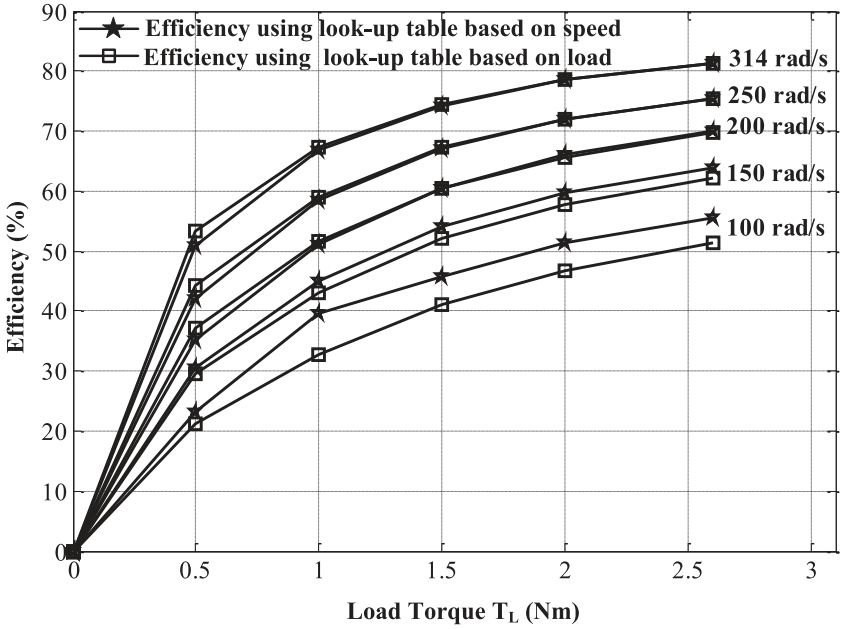

Fig. 6. Efficiency Vs load for look-up tables based on load and speed.

Please cite this article in press as: C.K. Lad, R. Chudamani, A simple overlap angle control strategy for reducing commutation torque ripple in a brushless DC motor drive, Eng. Sci. Tech., Int. J. (2017), https://doi.org/10.1016/j.jestch.2017.09.005

speed operation and it is clearly observed on electromagnetic torque encircled in Fig. 4(b) and (d). The increase in commutation torque ripple ΔT_e with speed showing its dependence on speed as well. Summarily, Figs. 3 and 4 show the dependence of commutation torque ripple on load as well as speed.

It is also observed that for light loads and lower speeds θ_{ov} can be made less than 15° to achieve a similar performance with that of TSDTC in which overlap angle is 15° fixed. Therefore an attempt has been made to find an optimum value of θ_{ov} for different loads and speeds. A logical conclusion for the estimation of θ_{ov} at different loads and speeds has been derived based on the simulation studies carried out keeping the goal as to suppress the commutation torque ripple within PWM torque ripple or to that in TSDTC. The following simulation results explain how the optimum value of θ_{ov} is finalized for the proposed method.

2.3.1. Simulation studies for fixed speed-variable load operation

In this study, the optimum overlap angle is determined for different load condition at fixed speed which suppresses commutation torque ripple within the PWM torque ripple or to that in TSDTC by trial and error. Similar procedure has been repeated with different speeds. Fig. 5(a) shows the group of curves of optimum overlap angle Vs load for different speeds. It can be observed that the overlap conduction of the motor is not required at low speed operation of 100 r/s. For speed of 130 r/s, overlap conduction is not required up to 1.75 Nm load. Afterwards optimum overlap angle increases to 3° at a load of 2.6 Nm. The increase in optimum overlap angle with increase in load and speed can be clearly observed from Fig. 5(a).

The worst case condition can be considered to fix the overlap angle for motor operation to reduce commutation torque ripple within PWM torque ripple for every speed of operation. Thus optimum overlap angle for 314 r/s operation can be considered to fix an overlap angle at different loads. The lookup table is prepared to obtain overlap angle for different values of load from no-load to full-load.

2.3.2. Simulation studies for fixed load-variable speed operation

In this study, the optimum overlap angle is determined in a similar manner as described above. Fig. 5(b) shows the group of curves of optimum overlap angle Vs speed for different loads. It can be observed from Fig. 5(b) that the overlap conduction of the motor is not required up to 116 r/s for any load. For a load of 0.5 Nm, overlap conduction is not required up to 150 r/s. Afterwards optimum overlap angle increases to 15° approx for a speed of 314 r/s. The increase in optimum overlap angle with increase in speed and load can be clearly observed from Fig. 5(b).

The worst case condition can be considered to fix the overlap angle for motor operation to reduce commutation torque ripple within PWM torque ripple for every load of operation. Thus the optimum overlap angle for 2.6 Nm load can be considered to fix the overlap angle at different speeds.

The look-up table prepared from fixed speed and variable load operation will be referred to as Look-up Table-I and that prepared from fixed load and variable speed operation as Look-up Table-II for further explanation. The Look-up Tables I & II

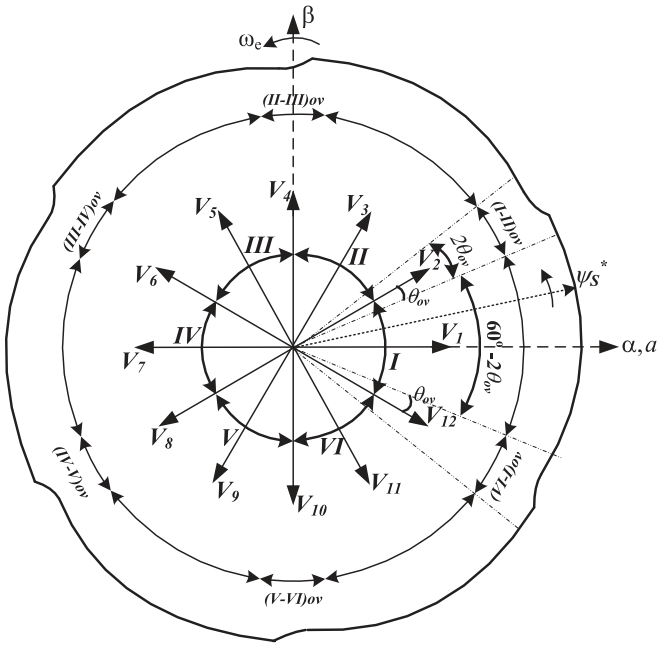

Fig. 8. Selection between non-overlap and overlap region for two and three phase conduction based on overlap angle θ_{ov} by proposed method.

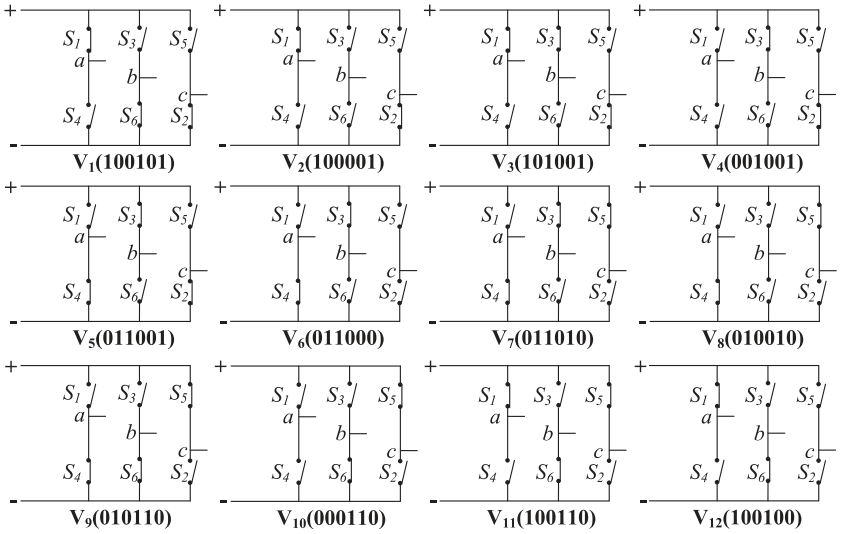

Fig. 7. Switching space vectors of inverter.

Please cite this article in press as: C.K. Lad, R. Chudamani, A simple overlap angle control strategy for reducing commutation torque ripple in a brushless DC motor drive, Eng. Sci. Tech., Int. J. (2017), https://doi.org/10.1016/j.jestch.2017.09.005

are prepared to fix an optimum overlap angle to reduce the commutation torque ripple to PWM ripple. Thus to finalize the optimum overlap angle, the drive efficiency is evaluated for both the aforesaid mode of operations. Fig. 6 shows the plot of efficiency Vs load for different speeds of operation. The efficiency obtained using Look-up Table-I and Look-up Table-II are compared. The condition for optimum overlap angle is derived from this comparison. From the efficiency curves it is clear that the values of θ_{ov} from Look-up Table-II gives optimum performance in the speed range of $\omega_m < 200$ r/s while it is achieved for $\omega_m > 200$ r/s using Look-up Table I.

2.4. Identification of overlap and non-overlap region

The switch combinations to realize twelve non-zero switching space vectors V_1, V_2 ….V_{12} are shown in Fig. 7. The binary code representation of all vectors from V_1 to V_{12} has been derived considering the switch sequence S_1, S_4, S_3, S_6, S_5, S_2. All odd numbered vectors correspond to three phase conduction of motor while all even numbered vectors correspond to two phase conduction of the motor.

The switching space vectors V_1, V_2 ….V_{12} are positioned at 30 electrical degrees apart as shown in Fig. 8. Conventional six sectors I-VI for SSDTC of BLDC are bound by all even numbered switching vectors V_2, V_4, ….V_{12} and all odd numbered vectors V_1, V_3….V_{11} for three phase conduction bisect the conventional sectors. Conventionally sectors are identified based on θ_e calculated in (13).

The proposed method suggests combined two and three phase conduction operation where the overlap angle is controlled according to the predetermined value. Thus motor is operated in three phase conduction mode between two

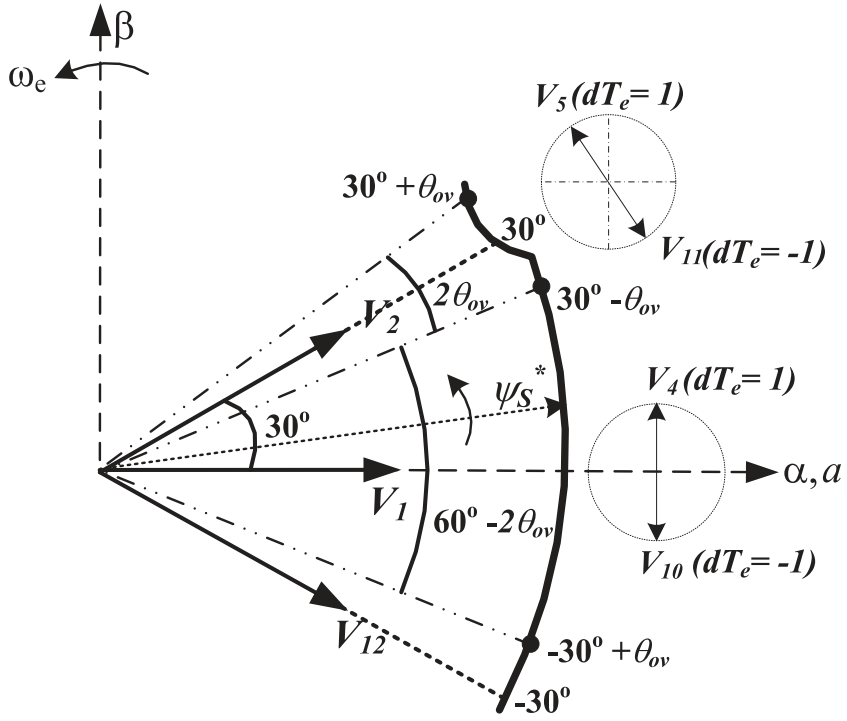

Fig. 9. Switching space vector selection for command vector ψ_s^* positioned in non-overlap region of sector I and overlap region $(I\text{-}II)_{ov}$ by proposed method.

Table 1
Twelve switching space vector selection for proposed method.

Sectors with non-overlap and overlap region	Position of the command vector	$d\psi_s = 0$			
		$dT_e = 1$		$dT_e = -1$	
		Vectors selected	Phase in conduction	Vectors selected	Phase in conduction
I	$-30+\theta_{ov}$ to $30-\theta_{ov}$	V_4	$b, -c$	V_{10}	$-b, c$
$(I-II)_{ov}$	$30-\theta_{ov}$ to $30+\theta_{ov}$	V_5	$-a, b, -c$	V_{11}	$a, -b, c$
II	$30+\theta_{ov}$ to $90-\theta_{ov}$	V_6	$-a, b,$	V_{12}	$a, -b$
$(II-III)_{ov}$	$90-\theta_{ov}$ to $90+\theta_{ov}$	V_7	$-a, b, c$	V_1	$a, -b, -c$
III	$90+\theta_{ov}$ to $150-\theta_{ov}$	V_8	$-a, c$	V_2	$a, -c$
$(III-IV)_{ov}$	$150-\theta_{ov}$ to $150+\theta_{ov}$	V_9	$-a, -b, c$	V_3	$a, b, -c$
IV	$150+\theta_{ov}$ to $-150-\theta_{ov}$	V_{10}	$-b, c$	V_4	$b, -c$
$(IV-V)_{ov}$	$-150-\theta_{ov}$ to $-150+\theta_{ov}$	V_{11}	$a, -b, c$	V_5	$-a, b, -c$
V	$-150+\theta_{ov}$ to $-90-\theta_{ov}$	V_{12}	$a, -b$	V_6	$-a, b,$
$(V-VI)_{ov}$	$-90-\theta_{ov}$ to $-90+\theta_{ov}$	V_1	$a, -b, -c$	V_7	$-a, b, c$
VI	$-90+\theta_{ov}$ to $-30-\theta_{ov}$	V_2	$a, -c$	V_8	$-a, c$
$(VI-I)_{ov}$	$-30-\theta_{ov}$ to $-30+\theta_{ov}$	V_3	$a, b, -c$	V_9	$-a, -b, c$

Please cite this article in press as: C.K. Lad, R. Chudamani, A simple overlap angle control strategy for reducing commutation torque ripple in a brushless DC motor drive, Eng. Sci. Tech., Int. J. (2017), https://doi.org/10.1016/j.jestch.2017.09.005

consecutive sectors and this region is identified as 'overlap region'. The motor operation with two phase conduction in the rest of the region identified as 'non-overlap region' of the sector as shown in Fig. 8. The command vector ψ_s^* is rotating in the direction of the motion. If it is passing through the non-overlap region of span $(60^\circ - 2\theta_{ov})$, two phase conduction takes place and when it is passing through the overlap region of span $2\theta_{ov}$, three phase conduction takes place. The overlap regions between two consecutive sectors $(I-II)_{ov}$, $(II-III)_{ov} \ldots (VI-I)_{ov}$ are shown in Fig. 8.

2.5. Selection of switching space vector for proposed method

The selection of switching space vector depends upon the position of the command vector ψ_s^* and output of hysteresis torque controller dT_e. Once the region is identified the '90° ahead' switching space vector in the direction of rotation is selected to increase the torque, while '90° behind' switching space vector in the opposite direction of rotation is selected to decrease the torque. Here BLDC motor operation is attempted for below base speed constant torque control.

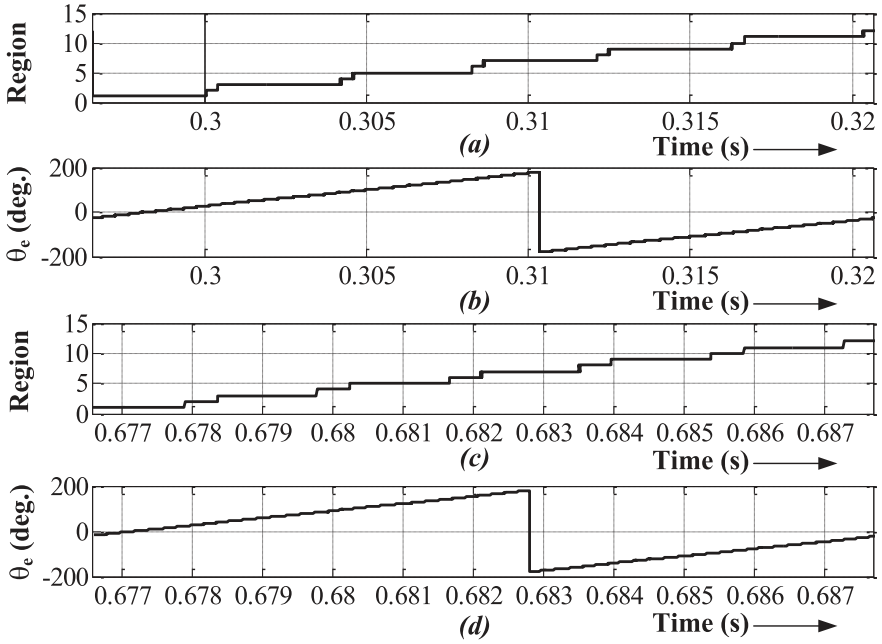

Fig. 10. Overlap and non-overlap region identification for proposed method (a) and (b) region and θ_e for 0.5 Nm, 130 r/s (c) and (d) region and for θ_e 0.5 Nm, 280 r/s.

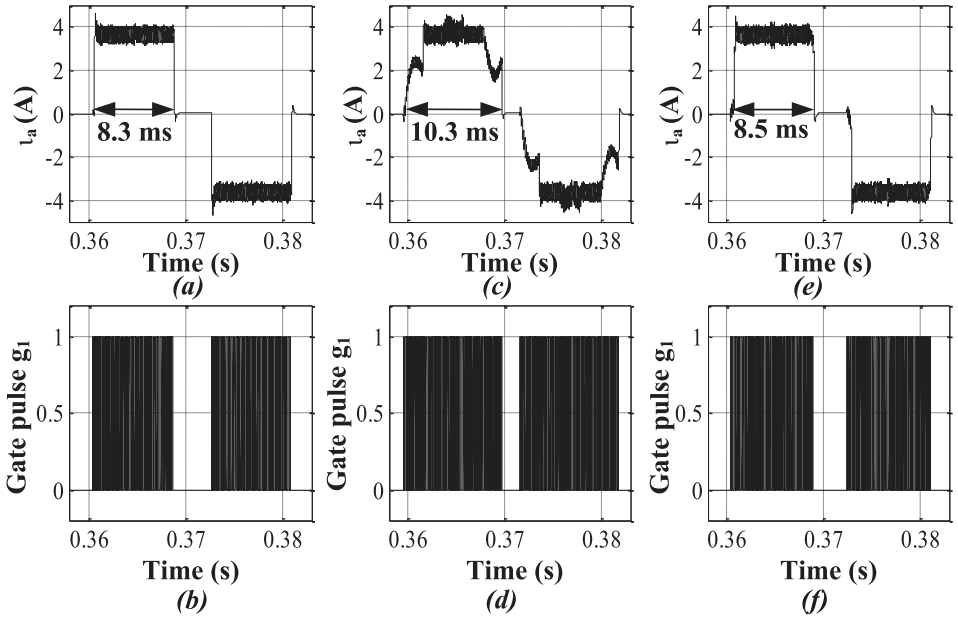

Fig. 11. Phase current and switching pulse respectively at 130 r/s and 2.6 Nm for (a) and (b) SSDTC, (c) and (d) TSDTC, (e) and (f) proposed method.

Please cite this article in press as: C.K. Lad, R. Chudamani, A simple overlap angle control strategy for reducing commutation torque ripple in a brushless DC motor drive, Eng. Sci. Tech., Int. J. (2017), https://doi.org/10.1016/j.jestch.2017.09.005

Fig. 9 depicts the selection of switching space vector by the proposed method. When the command vector ψ_s^* is positioned between $(-30^\circ + \theta_{ov})$ to $(30^\circ - \theta_{ov})$ of non-overlap region of sector-I, switching space vector V_4 is switched to produce accelerating torque while vector V_{10} is switched to produce decelerating torque. Here V_4 and V_{10} switching result in two phase conduction. When the command vector ψ_s^* shifts to overlap region between $(30^\circ - \theta_{ov})$ to $(30^{\text{deg}} + \theta_{ov})$ of span $2\theta_{ov}$, accelerating vector V_5 and decelerating vector V_{11} are switched which lead to three phase conduction. Similarly the command vector ψ_s^* consecutively changes position between non-overlap and overlap region, the switching space vectors are selected as given in Table 1. The Table 1 is derived by assuming constant flux control hence only torque error is considered for switching vector selection. The '–' sign before the phases in conduction indicates the direction of current. In the following section the performance of the drive for various operating conditions are simulated and the results are discussed.

3. Simulation results

The simulations are carried out for comparative studies using (i) SSDTC, (ii) TSDTC and (iii) proposed DTC of BLDC motor. The simulations are carried out in MATLAB/Simulink® environment. The proposed method is compared with other two methods.

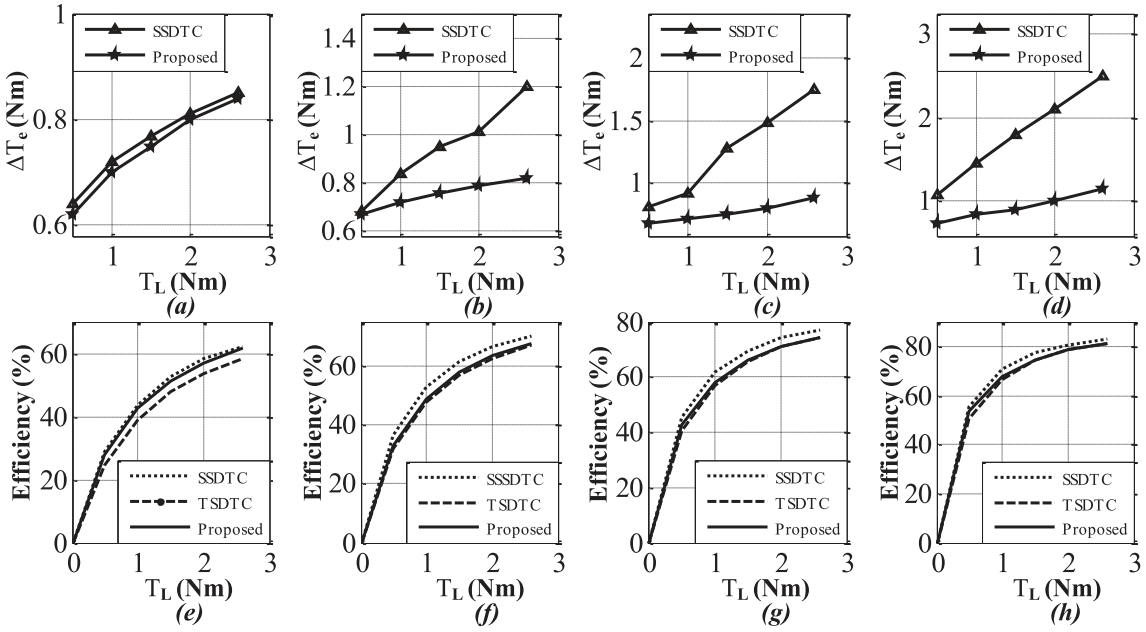

Fig. 12. Commutation torque ripple ΔT_e Vs load and drive efficiency Vs load respectively for (a) and (e) 130 r/s, (b) and (f) 180 r/s, (c) and (g) 240 r/s, (d) and (h) 314 r/s.

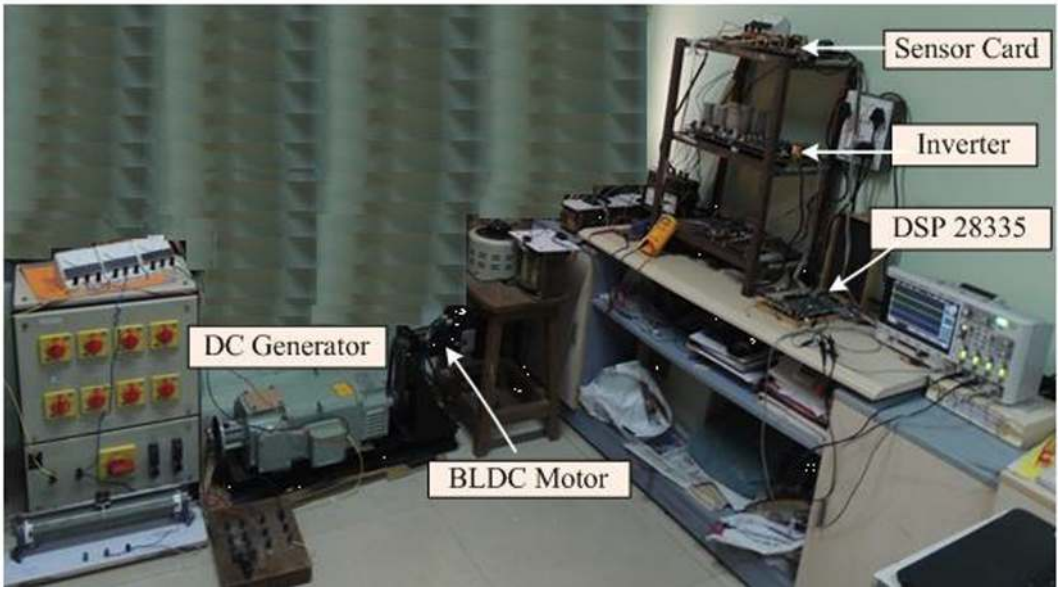

Fig. 13. Experimental Setup.

Please cite this article in press as: C.K. Lad, R. Chudamani, A simple overlap angle control strategy for reducing commutation torque ripple in a brushless DC motor drive, Eng. Sci. Tech., Int. J. (2017), https://doi.org/10.1016/j.jestch.2017.09.005

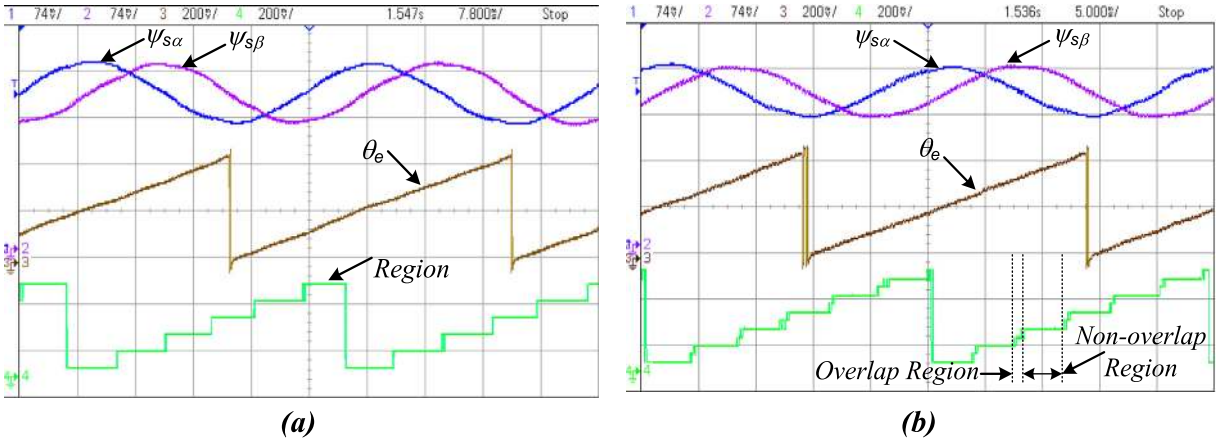

Fig. 14. Experimental result of Stator flux linkages, θ_e and region identification at no-load for (a) 84 r/s and (b) 126 r/s.

Parameters of BLDC motor considered for simulation study are same as parameters of motor used in experimentation and are given in Appendix A.

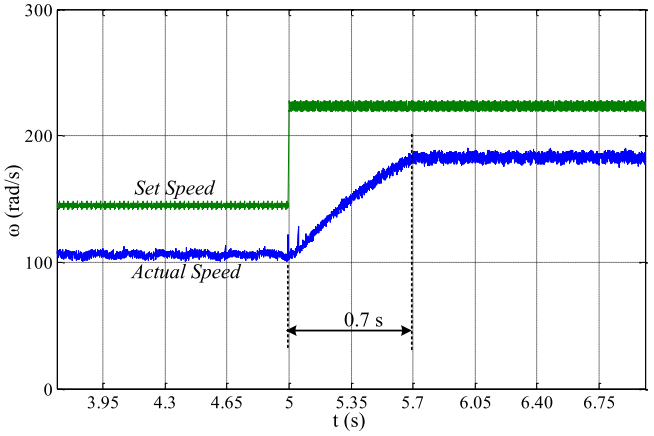

Fig. 15. Drive operation for step change in speed from 104 r/s to 188 r/s.

The effect of load and speed on the overlap angle is shown in Fig. 10, which shows the increase in overlap region for higher speeds.

In the proposed method the commutation torque ripple is suppressed by determining optimum overlap angle based on speed and load. It controls the span of phase conduction in between 120° to 150°.

Fig. 11 shows phase 'a' current and switching pulse of device 'S_1' for one electrical cycle for SSDTC, TSDTC and proposed method for low speed operation. It can be observed that phase conduction period is 8.3 ms for SSDTC in Fig. 11(a) while it is 10.3 ms for TSDTC in Fig. 11(c). Due to low speed operation overlap angle is small and the operation is almost similar to SSDTC. The conduction period of 8.5 ms in the proposed method is almost equal to SSDTC. Longer the conduction period higher will be the winding losses and the switching losses will be higher due to increased numbers of switching.

The steady state performance of the drive for low speed and high speed operation in terms of commutation torque ripple ΔT_e and drive efficiency is evaluated and simulation results are presented. The torque ripple ΔT_e for different speeds are plotted for SSDTC and proposed method in Fig. 12(a)-(d) while the drive effi-

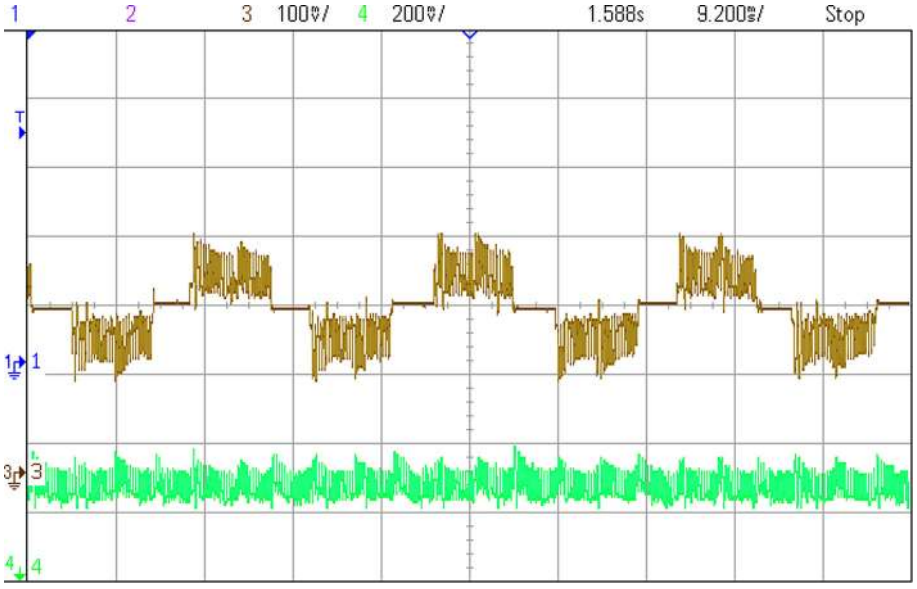

Fig. 16. Phase-'a' current (2 A/div) and electromagnetic torque (0.347 Nm/div) for drive operation at 126 r/s and 0.55 Nm load.

Please cite this article in press as: C.K. Lad, R. Chudamani, A simple overlap angle control strategy for reducing commutation torque ripple in a brushless DC motor drive, Eng. Sci. Tech., Int. J. (2017), https://doi.org/10.1016/j.jestch.2017.09.005

ciency curves for the same set of speeds using the proposed method are plotted and compared with that of SSDTC and TSDTC in Fig. 12(e)-(h).

For lower and higher speeds as well as wide range of the load, attempt has been made to keep the commutation torque ripple within the PWM torque ripple or that in TSDTC. From the ΔT_e plot in Fig. 12(a) it is observed that the proposed method gives reduced torque ripple equal to that in TSDTC for low speed operation while maintaining the drive efficiency equal to that in SSDTC in Fig. 12(e). For higher speeds as the overlap angle increases the efficiency could not be maintained equal to SSDTC but it is higher than TSDTC with equal reduction in commutation torque ripple to that in TSDTC.

4. Experimental results

The proposed overlap angle controlled DTC scheme of a BLDC motor drive have been evaluated using experimental setup shown in Fig. 13. The proposed control algorithm is implemented using DSP TMS320F28335. BLDC motor parameters are given in an Appendix and same motor parameters are used in simulation studies.

Initially motor performance is verified for two different speeds of 84 r/s and 126 r/s at no-load. The stator flux linkages $\psi_{s\alpha}$ and $\psi_{s\beta}$, θ_e estimated and regions are observed in Fig. 14. Due to low speed operation, no effect of overlap angle is observed in regions in Fig. 14(a), they are as similar as sectors of SSDTC. For increased

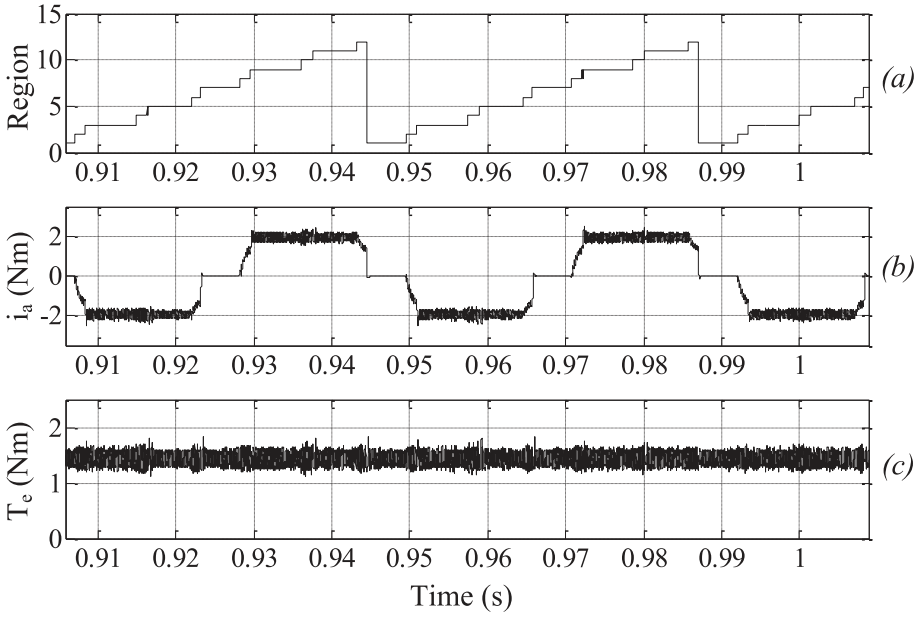

Fig. 17. Simulation results for proposed method (a) region identification, (b) Phase-'a' current and (c) electromagnetic torque for drive operation at 74 r/s and 1.4 Nm load.

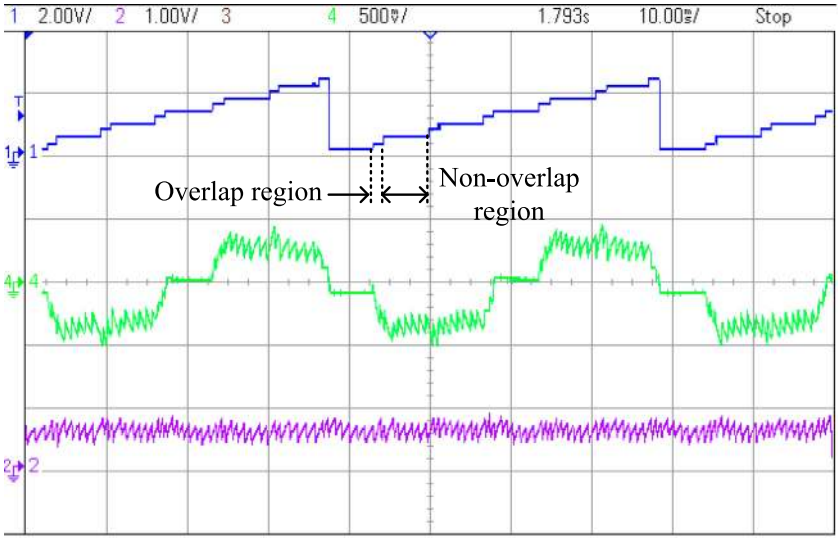

Fig. 18. Experimental results for proposed method: Region identification, Phase-'a' current (2 A/div) and electromagnetic torque (2 Nm/div) for drive operation at 74 r/s and 1.4 Nm load.

Please cite this article in press as: C.K. Lad, R. Chudamani, A simple overlap angle control strategy for reducing commutation torque ripple in a brushless DC motor drive, Eng. Sci. Tech., Int. J. (2017), https://doi.org/10.1016/j.jestch.2017.09.005

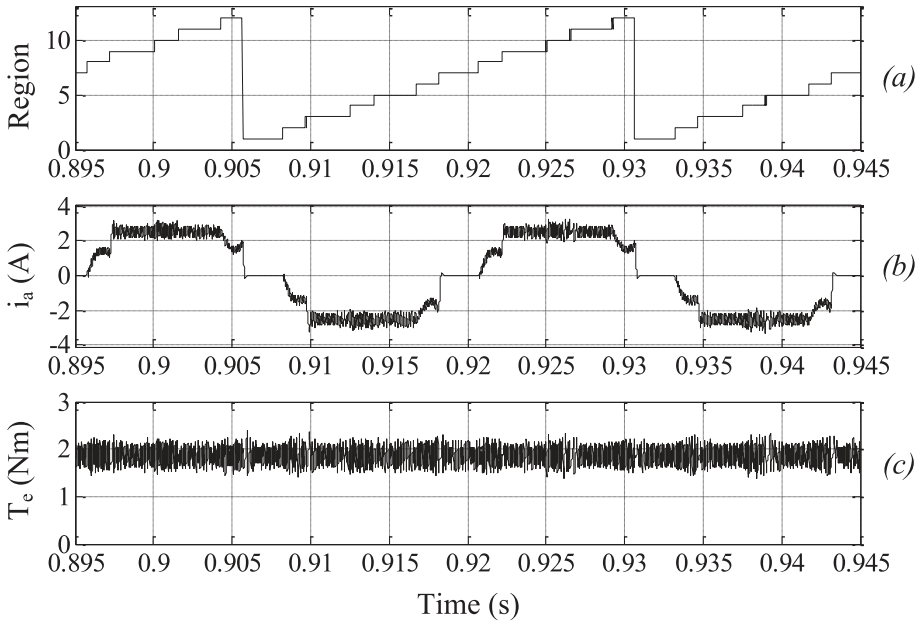

Fig. 19. Simulation results for proposed method (a) region identification, (b) Phase-'a' current and (c) electromagnetic torque for drive operation at 126 r/s and 1.8 Nm load.

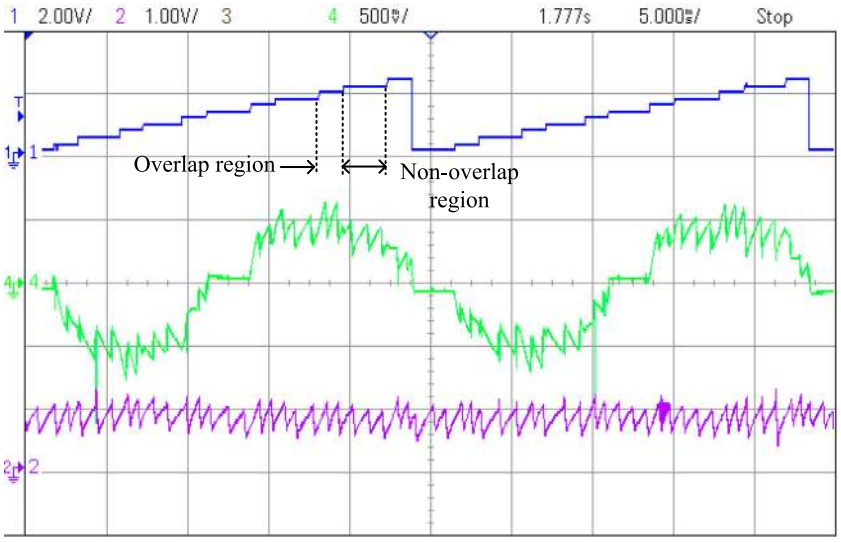

Fig. 20. Experimental results for proposed method: Region identification, Phase-'a' current (2 A/div) and electromagnetic torque (2 Nm/div) for drive operation at 126 r/s and 1.8 Nm load.

speed of 126 r/s, the overlap angle is obtained from look-up table and small overlap region appears in region identification in Fig. 14(b).

The speed control of the BLDC drive for proposed method is verified experimentally. The 2000 ppr inbuilt encoder signal is given to the capture unit of DSP processor for speed measurement. A step change is applied in speed from 104 r/s to 188 r/s. The motor attained set speed in 0.7 s after step change can be observed in Fig. 15. A separately excited DC generator is coupled with BLDC motor for loading. The phase current and estimated torque of motor for 120 r/s and 0.55 Nm load are shown in Fig. 16. As commutation torque ripples are effectively suppressed only pwm torque ripples appear in developed torque. For torque control sampling time of 75 μs is chosen while hysteresis band of 0.001 Nm is set for torque controller.

The drive performance is verified by simulation studies as well as experimental investigation for different speed and load applied. Figs. 17 and 18 show simulation and experimental results for drive operation at 74 r/s and 1.4 Nm load. An overlap angle of 6° is determined from the look-up table. The effect of the overlap conduction is observed over phase commutation and commutation torque ripple for the load applied. Similar has been verified for increase in speed and load to 126 r/s and 1.8 Nm respectively as shown in Figs. 19 and 20. In this case, the overlap angle is increased to 11° which increases span of overlap region. As can be observed from Fig. 17 to Fig. 20, the commutation torque ripple is effectively suppressed by proposed method using overlap angle control for applied speed and load conditions.

The conduction period and inverter device switching for proposed method is evaluated from Figs. 21 and 22 for drive operation

Please cite this article in press as: C.K. Lad, R. Chudamani, A simple overlap angle control strategy for reducing commutation torque ripple in a brushless DC motor drive, Eng. Sci. Tech., Int. J. (2017), https://doi.org/10.1016/j.jestch.2017.09.005

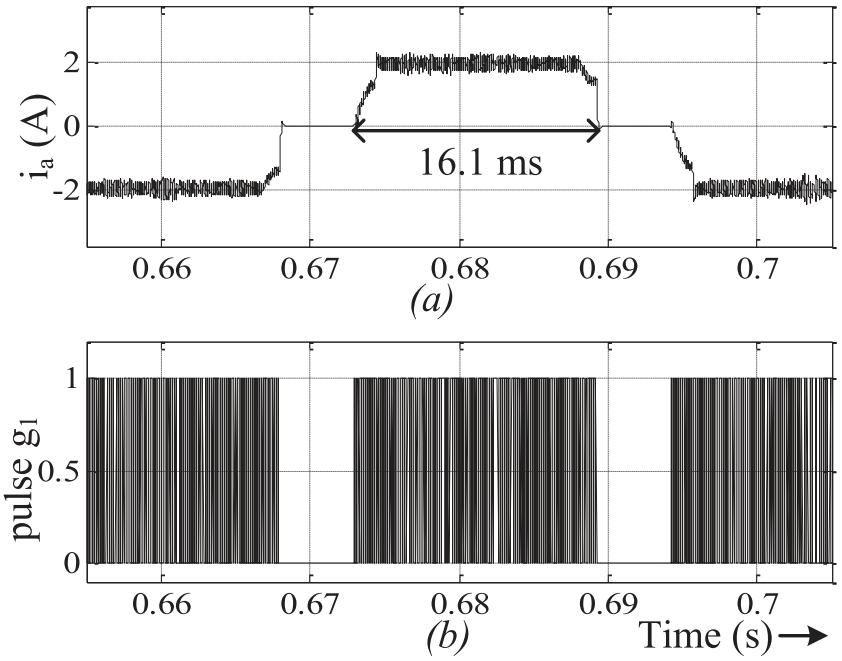

Fig. 21. Simulation results of phase 'a' current and switching pulses for proposed method at 74 r/s and 1.4 Nm load.

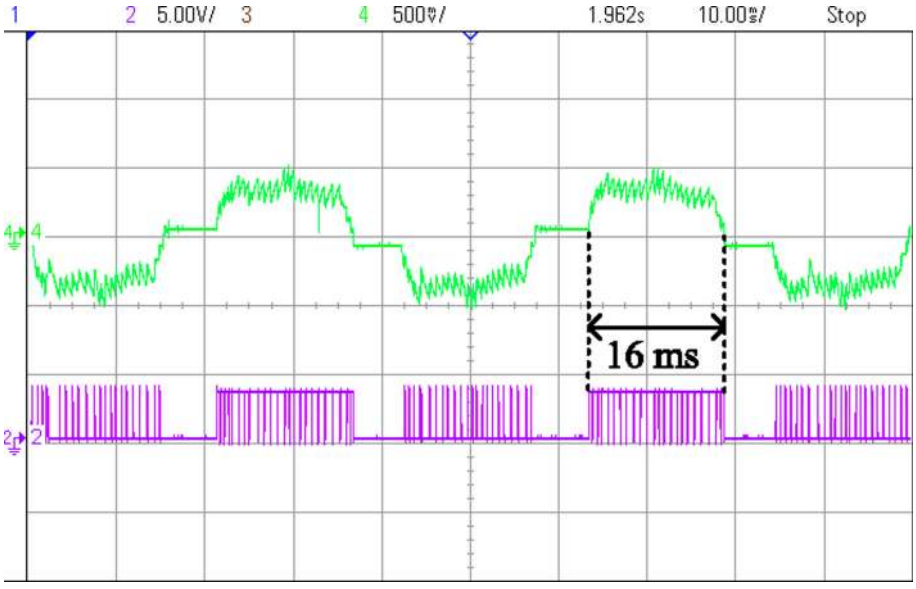

Fig. 22. Experimental results of phase 'a' current (2 A/div) and switching pulses for proposed method at 74 r/s and 1.4 Nm load.

at 74 r/s and 1.4 Nm load applied. The conduction period for a half cycle of phase current is observed to be 16.1 ms and 16 ms in simulation and experimental results respectively. From the results presented above, it is observed that the experimental results match with the simulation results obtained for the proposed method.

5. Conclusions

The combined two and three phase conduction DTC of BLDC motor with overlap angle control is proposed in this paper. The proposed method is compared with SSDTC and TSDTC. The increased number of switching space vector effectively reduces commutation interval and magnitude of commutating current, thus reducing the commutation torque ripple. To determine optimum overlap angle the effect of commutation on motor performance is studied for wide range of speed and load individually. The characteristics of optimum overlap angle are determined with respect to load and speed to suppress the commutation torque ripple. Further both the characteristics are analysed for the drive efficiency. Finally looking towards the optimum performance (minimum ΔT_e and maximum efficiency), a look-up table is derived to find optimum overlap angle to reduce commutation torque ripple within PWM ripples or that produced in TSDTC. The drive performance is evaluated for transient and steady state performance at different speeds and loads using the proposed method. The commutation torque ripple is considerably reduced

Please cite this article in press as: C.K. Lad, R. Chudamani, A simple overlap angle control strategy for reducing commutation torque ripple in a brushless DC motor drive, Eng. Sci. Tech., Int. J. (2017), https://doi.org/10.1016/j.jestch.2017.09.005

by proposed method in comparison with SSDTC with optimum overlap conduction. The winding losses are reduced by reducing the conduction period. Further the inverter losses are reduced by reducing the numbers of switching of the devices of inverter in the proposed method in comparison with TSDTC. Its effect is observed on the drive efficiency. The proposed method gives optimized operation between SSDTC and TSDTC.

The proposed method has been implemented in hardware and the simulation results are validated.

Appendix A

Parameters of BLDC motor

DC supply	310 V
Numbers of pole	4
Stall current	4.3 A
Peak current	12.9 A
Continuous stall torque	3.2 Nm
Peak torque	9.6 Nm
Stator resistance per phase	1.79Ω
Stator inductance per phase	4.565 mH
Rated speed	3000 rpm (314 r/s)
Back-EMF constant	78 V_{peak} (L-L)/krpm
Toque constant	0.74 Nm/A-peak
Inertia	0.00029 kg-m^2
Friction Factor	0.000506 Nm/r/s

References

[1] R. Krishnan, Electric Motor Drives: Modeling, Prentice Hall of India, Analysis and Control, 2002.
[2] B.K. Bose, Modern Power Electronics and AC Drives, Prentice Hall, PTR, 2002.
[3] J. Hung, Z. Ding, Design of currents to reduce torque ripple in brushless permanent magnet motors, in: IEE Proceedings B-Electric Power Applications, 1993, pp. 260–266.
[4] C.-S. Berendsen, G. Champenois, A. Bolopion, Commutation strategies for brushless DC motors: influence on instant torque, IEEE Trans. Power Electron. 8 (1993) 231–236.
[5] T.M. Jahns, Torque production in permanent-magnet synchronous motor drives with rectangular current excitation, in: IEEE Transactions on Industry Applications, 1984, pp. 803–813.
[6] J.W. Dixon, L. Leal, Current control strategy for brushless DC motors based on a common DC signal, IEEE Trans. Power Electron. 17 (2002) 232–240.
[7] J.-H. Song, I. Choy, Commutation torque ripple reduction in brushless DC motor drives using a single DC current sensor, IEEE Trans. Power Electron. 19 (2004) 312–319.
[8] T. Hui, Controllability analysis of torque ripple due to phase commutation in brushless DC motors, in: ICEMS 2001 Proceedings of the Fifth International Conference on Electrical Machines and Systems, 2001, pp. 1317–1322.
[9] W. Hu, Q. Li, The analysis of evolution and ripple of torque during the phase commutation in brushless dc motor, in: ICEMS 2003 Sixth International Conference on Electrical Machines and Systems, 2003, pp. 202–204.
[10] B.-H. Kang, C.-J. Kim, H.-S. Mok, G.-H. Choe, Analysis of torque ripple in BLDC motor with commutation time, in: Proceedings. ISIE 2001. IEEE International Symposium on Industrial Electronics, 2001, pp. 1044–1048.
[11] Y.-K. Lin, Y.-S. Lai, Pulsewidth modulation technique for BLDCM drives to reduce commutation torque ripple without calculation of commutation time, IEEE Trans. Ind. Appl. 47 (2011) 1786–1793.
[12] N. Saha, S. Panda, Speed control with torque ripple reduction of switched reluctance motor by Hybrid Many Optimizing Liaison Gravitational Search technique, Eng. Sci. Technol., Int. J. (2016).
[13] S. Bharatkar, R. Yanamshetti, D. Chatterjee, A. Ganguli, Commutation torque ripple analysis and reduction through hybrid switching for BLDC motor drives, in: 2008. ICIIS 2008. IEEE Region 10 and the Third international Conference on Industrial and Information Systems, 2008, pp. 1–5.
[14] I. Kim, N. Nakazawa, S. Kim, C. Park, C. Yu, Compensation of torque ripple in high performance BLDC motor drives, Control Eng. Practice 18 (2010) 1166–1172.
[15] R. Carlson, M. Lajoie-Mazenc, J. Fagundes, Analysis of torque ripple due to phase commutation in brushless DC machines, IEEE Trans. Ind. Appl. 28 (1992) 632–638.
[16] T. Shi, Y. Cao, G. Jiang, X. Li, C. Xia, A torque control strategy for torque ripple reduction of brushless DC motor with non-ideal back electromotive force, IEEE Trans. Industr. Electron. (2017).
[17] D.-K. Kim, K.-W. Lee, B.-I. Kwon, Commutation torque ripple reduction in a position sensorless brushless DC motor drive, IEEE Trans. Power Electron. 21 (2006) 1762–1768.
[18] H. Lu, L. Zhang, W. Qu, A new torque control method for torque ripple minimization of BLDC motors with un-ideal back EMF, IEEE Trans. Power Electron. 23 (2008) 950–958.
[19] L. Zhong, M.F. Rahman, W.Y. Hu, K. Lim, Analysis of direct torque control in permanent magnet synchronous motor drives, IEEE Trans. Power Electron. 12 (1997) 528–536.
[20] Y. Liu, Z. Zhu, D. Howe, Direct torque control of brushless DC drives with reduced torque ripple, IEEE Trans. Ind. Appl. 41 (2005) 599–608.
[21] Y. Liu, Z.Q. Zhu, D. Howe, Commutation-torque-ripple minimization in direct-torque-controlled PM brushless DC drives, IEEE Trans. Ind. Appl. 43 (2007) 1012–1021.
[22] J. Gao, Y.-W. Hu, W.-X. Huang, Z.-F. Huang, The Direct Self Control of Brushless DC Motor Based on the Hexagon Locus of Stator Flux Linkage, in: Zhongguo Dianji Gongcheng Xuebao(Proceedings of the Chinese Society of Electrical Engineering), 2007, pp. 64–69.
[23] J. Yang, Y. Hu, W. Huang, J. Chu, J. Gao, Direct torque control of brushless DC motor without flux linkage observation, in: Power Electronics and Motion Control Conference, 2009. IPEMC'09. IEEE 6th International, 2009, pp. 1934–1937.
[24] Y. Li, J. Ma, J. Liu, Q. Yu, D. Zhang, J. Guan, et al., Study on the use of zero voltage vectors in the PMSM DTC system, in: Control Conference (CCC), 2011 30th Chinese, 2011, pp. 3559–3564.
[25] S.B. Ozturk, H.A. Toliyat, Direct torque control of brushless dc motor with non-sinusoidal back-EMF, in: Electric Machines & Drives Conference, 2007. IEMDC'07 IEEE International, 2007, pp. 165–171.
[26] M. Noroozi, J. Moghani, J.M. Monfared, H. Givi, An improved direct torque control of brushless DC motors using twelve voltage space vectors, in: Power Electronics and Drive Systems Technology (PEDSTC), 2012 3rd, 2012, pp. 133–138.
[27] M. Masmoudi, B. El Badsi, A. Masmoudi, Direct torque control of brushless DC motor drives with improved reliability, IEEE Trans. Ind. Appl. 50 (2014) 3744–3753.

Please cite this article in press as: C.K. Lad, R. Chudamani, A simple overlap angle control strategy for reducing commutation torque ripple in a brushless DC motor drive, Eng. Sci. Tech., Int. J. (2017), https://doi.org/10.1016/j.jestch.2017.09.005